Influence of Three-Dimensional Fibrotic Patterns on Simulated Intracardiac Electrogram Morphology

Matthias W Keller[1], Armin Luik[2], Mohammad Soltan Abady[1], Gunnar Seemann[1], Claus Schmitt[2], Olaf Dössel[1]

[1] Institute of Biomedical Engineering, Karlsruhe Institute of Technology, Karlsruhe, Germany
[2] Städtisches Klinikum Karlsruhe, Karlsruhe, Germany

Abstract

Complex fractionated atrial electrograms (CFAE) are a target for catheter ablation as they coincide with areas of slow conduction. In this study we simulated different volume fractions of diffuse and patchy fibrosis up to 50 %. Catheter signals for different electrode spacings were calculated and characteristic features were compared to a clinical database of CFAE-signals. A linear slowing of global conduction velocities was found independent of the type of fibrosis. For patchy fibrosis, electrograms displayed fractionation, which was not seen for diffuse fibrosis of the same degree. In comparison to clinical data, simulated electrograms showed up to 10 zero crossings per electrogram, which was also seen for clinical EGMs with medium fractionation (class 2 of 3). For both, clinical (84 %) and simulated (88 %) signals, a significant difference in amplitude is present between fractionated and non-fractionated signals.

1. Introduction

Catheter ablation based treatment of atrial fibrillation (AF) has become a major technique in todays clinical procedures. Trigger and substrate are most frequently discussed mechanisms for initiation and perpetuation of AF. Whereas trigger elimination by isolating the pulmonary veins is already established, the discussion about the right mapping strategy is ongoing. Complex fractionated electrograms (CFAE) are described as a promising target for ablation [1]. The genesis of these electrograms (EGM), which is still unclear, is often associated with fibrosis. It has been shown that highly fibrotic areas cause a conduction delay, which can maintain AF [2]. Spacing of catheter electrodes, used to record CFAE, varies between 1 mm to 5 mm edge to edge distance. Usually bipolar signals are regarded as they are less tainted with farfield.

Up to today, several studies are available simulating EGMs on fibrotic areas. In [2] and [3] EGMs for a microstructure approach containing a 2D-layer of cells randomly uncoupled by strand like fibrotic elements are presented. Campos et al. [4] investigated effects of fibrosis using a histological model. They extended their one slice setup by a second layer containing only major fibrotic obstacles in order to allow excitation spread below and around fibrotic elements. Limitation of these studies is the quasi 2D-setting, as intracardiac EGMs reflect the summed potentials from a three dimensional area underneath and surrounding the measuring electrodes. Clinical catheters have electrodes of a distinct size, leading to spatial averaging and therefore smoothing of recorded signals.

In this study we investigated the influence of varations in 3D myocardial structure regarding conduction propagation and EGM alterations. Thereby, we try to contribute to the discussion if it is reasonable to ablate CFAE areas because they are hiding fibrotic substrates. We created setups representing patchy and diffuse fibrosis with different degrees of fibrotic volume fraction (VFr). For clinical verification, simulated EGM were compared with characteristic features extracted from an annotated clinical database of 605 CFAE signals, which was presented in [5]. Features, as e.g. the number of zero crossings per EGM were chosen to study morphology and temporal behavior.

2. Methods

2.1. Calculation of cardiac potentials

Cardiac excitation was calculated using the monodomain equation (eq. 1). Aiming at the calculation of extracellular potentials, the received transmembrane currents served as an input for the forward calculation based on equation 2. A previous study has shown, that this computationally less expensive method delivers EGMs with a reasonable precision, however it underestimates the width of the wavefront and leads to a decreased EGM width [6].

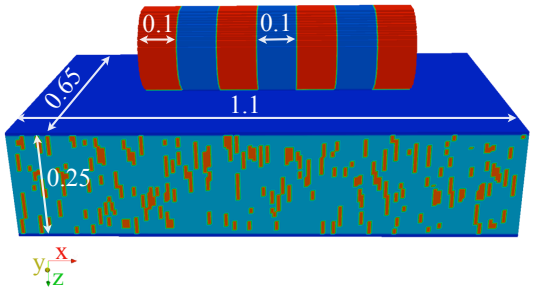

Figure 1. Simulation setup 1, containing a four electrode catheter, and patchy fibrosis with a VFr of 30%. Indicated numbers represent dimensions in cm.

$$\nabla \cdot (\sigma_M \nabla V_m) = \beta(C_m \frac{dV_m}{dt} + I_{mem}) = \beta I_m \qquad (1)$$

with the bulg conductivity $\sigma_M = 0.245\,\mathrm{S/m}$, the transmembrane voltage V_m and cell-surface to volume ratio β.

$$-\nabla \cdot (\sigma_e \nabla \phi_e) = \beta I_m \qquad (2)$$

Bipolar EGMs $V_{bip}(t)$ were calculated as the difference of $\phi_{e,p}(t)$ and $\phi_{e,d}(t)$ (the potentials on the proximal and distal catheter electrode). To describe atrial cellular behavior the Courtemanche-Ramirez-Nattel model was chosen [7].

2.2. Geometry

Simulations of catheter signals for different fibrosis geometries (diffuse, patchy) were performed on regular spaced grid of cubic elements with a spatial resolution of 50 μm. Each setup included a plane sheet of myocardium (length: 1.1 cm, width: 0.65 cm, thickness: 0.25 cm) covered by a passive layer of endothelium and one of two different catheter geometries. We modeled the catheter by electrodes as areas of high conductivity ($\sigma_{el} = 700\,\mathrm{S/m}$), separated by electrically isolating material ($\sigma_{is} = 10^{-22}\,\mathrm{S/m}$). Catheter diameter was 2.3 mm, which is equivalent to 7 F. Electrode width was 1 mm and spacing varied between 1-5 mm edge to edge (see figure 1) .

2.3. Modeling fibrosis

We created diffuse and patchy fibrosis patterns as presented in [8]. Seed points for fibrotic elements were randomly distributed. For x, y and z coordinates a uniform distribution was assumed. For diffuse patterns we placed a fibrotic cube of 2x2x2 voxels at each seed point. In case of patchy fibrosis disk like elements were positioned. The size of these disks was described by a fixed width of 2 voxels (x-direction for most cases) and two parameters (y- and z-length) were described by Poisson distributions with

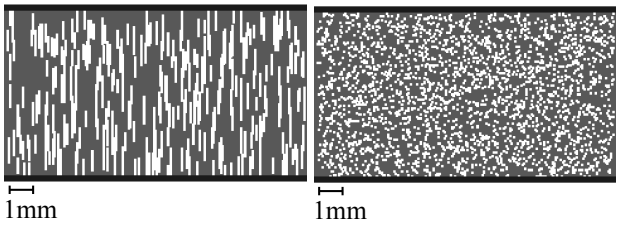

Figure 2. Exemplary 2D views on x-y-plane of fibrotic tissue; VFr 30 %; Right: Patchy fibrosis; Left: Diffuse fibrosis.

$\lambda_y = 900\,\mu\mathrm{m}$ as suggested in [2], [3]. Related to the reduced tissue thickness in z-direction, $\lambda_z = 300\,\mu\mathrm{m}$ was assumed. Elements were created until the set VFr was reached (fig. 2). Fibrotic elements were treated as electrically isolating and passive elements. The aim of this study was to determine the influence of collagenous structures on conduction velocity (CV) and EGM shape. Therefore tissue conductivity and sodium handling was not varried as described in other studies [3].

2.4. Comparison to CFAE database

For comparison to clinical values we extracted several characteristic signal parameters from a database of 605 CFAE and non-fractionated bipolar signals, with a length of 5 s each. All signals have been annotated by experienced electrophysiologists and referred to one of four classes ranging from CFAE 0 for non fractionated signals to CFAE 3 for continuous activity. Clinical signals are filtered by a standard clinical bandpass filter (30-250 Hz). For a detailed description of the database, see [5]. We segmented each signal in active and inactive segments using an adaptive thresholding algorithm described in [9]. For each segment, the peak to peak amplitude (PPA), the number and temporal distance of zero crossings (NZC, TZC), as well as the number of positive maxima and their temporal distance (NM, TM) were extracted. We used the same algorithm to characterize the simulated EGMs.

3. Results

Patterns of diffuse and patchy fibrosis could be created using random distributions. For each type of fibrosis global CV was extracted and the corresponding bipolar EGM were simulated. EGM were then analyzed for characteristic features and compared to a clinical CFAE database.

3.1. Conduction velocity

We calculated global CV for each simulation. The results for both types of fibrosis over fibrotic VFr are shown in figure 3. A nearly linear relationship for CV independent of the type of fibrosis can be seen.

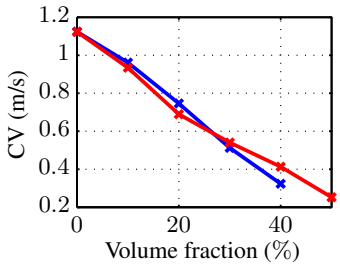

Figure 3. Development of global CV for increasing fibrotic VFrs; Diffuse fibrosis (blue), patchy fibrosis (red). For 50 % diffuse fibrosis conduction block occured.

3.2. Diffuse fibrosis

For several VFr of diffuse fibrosis, we simulated EGM for catheters with different electrode spacings. In figure 4 unfiltered and filtered signals for VFr up to 40 % are displayed. For a simulation with a VFr of 50 % conduction block occurred. Unfiltered signals show a decrease in amplitude as well as an increase in EGM width, which can be related to conduction slowing, shown above. Although a slightly serrated signal shape is visible for higher degrees of fibrosis, no fractionation occurred. Clinical filtering led to a symmetric relationship of positive and negative amplitude and restored smooth shape of signals.

3.3. Patchy fibrosis

In our simulations, a patchy geometry of fibrosis led to pronounced changes in signal morphology. For increasing VFr of fibrosis, a transition from the triphasic morphology seen without fibrosis (see fig. 4) to a low amplitude and highly fractionated shape is visible (fig. 5). Applying a clinical filter leads to a signal smoothing. However the major peaks are preserved. Clear fractionation started at a fibrotic VFr of 30 %. In order to study the influence of orientation of fibrotic elements, two signals for a patchy VFr of 30 % are displayed in figure 6. One signal was received for a parallel orientation of fibrotic elements, showing a smooth not-fractionated course. The other, fractionated signal is a result from an orthogonal orientation.

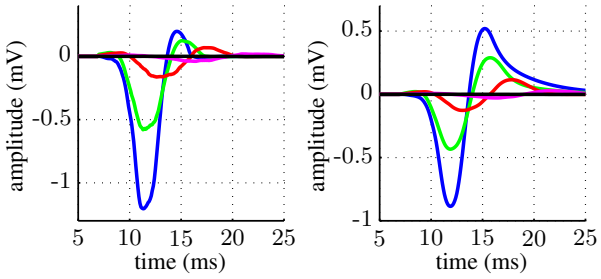

Figure 4. Bipolar signals measured on a myocardial patch containing different VFr of diffuse fibrosis: 0 % (blue), 10 % (green), 20 % (red), 30 % (magenta), 40% (black); left: unfiltered signals; right: filtered signals

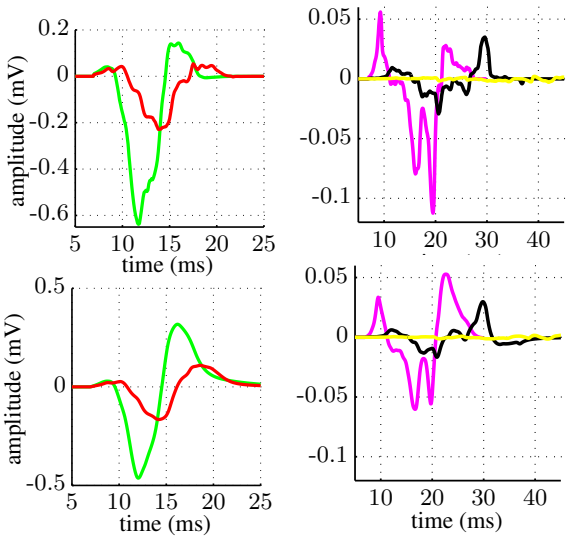

Figure 5. Bipolar signals measured on a myocardial patch containing different VFrs of patchy fibrosis: 10 % (green), 20 % (red), 30 % (magenta), 40 % (black), 50% (yellow); (for 0 % see figure 4); top: unfiltered signals; bottom: filtered signals;

3.4. Comparison to clinical data

Characteristic features extracted from our clinical database as well as from simulated signals are shown in tables 1 and 2. Simulated signals were evaluated for three different electrode spacings (1, 3, 5 mm) and filtered before analysis, to be comparable to clinical signals. For clarity, table 2 only shows values of EGMs for VFrs of 0 % (no fractionation) and 30-50 % (fractionation) for patchy fibrosis, which are comparable to classes CFAE0 and CFAE1, 2. Clinical data show a reduction in peak to peak amplitude of 5 mV from 5.53 mV for CFAE0 to 0.86 mV (relative chage: 84 %) for CFAE1 comparing fractionated and non fractionated EGMs. For simulated EGM a change from 1.07 mV to 0.12 mV for the first frac-

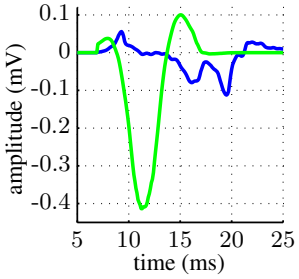

Figure 6. Bipolar signals for different orientations of patchy fibrosis relative to propagation direction; Parallel orientation (green), orthogonal orientation (blue)

Table 1. Characteristic features extracted from the CFAE Database; CFAE 0: no fractionation, CFAE 3: continuos activity; PPA: peak to peak amplitude (mV); NM/Z: number of maxima/ zero crossings; TM/Z: mean time (ms) between maxima/ zero crossings;

	PPA	NM	TM	NZC	TZC
CFAE 0	5.53	3.67	12.73	4.60	10.63
CFAE 1	0.86	4.84	14.55	6.21	11.54
CFAE 2	0.78	8.14	14.25	10.45	11.21
CFAE 3	0.63	21.04	14.90	26.07	11.96

tionated EGMs (VFr 30 %, relative change: 88 %) takes place. Regarding the number of zero crossings, simulated signals display two zero crossings per EGM for VFr of 0 % up to ten for a VFr of 50 % and an electrode spacing of 5 mm. The latter is in the range of class CFAE2 for the clinical signals. Development for the number of maxima is similar. Regarding the time between zero crossings, clinical signals are in the range between 10.63 ms and 11.96 ms comparing to 5-8 ms for simulated signals.

4. Discussion and conclusions

Our 3D simulation study showed a linear decrease of CV with increased fibrotic VFr, independent of fibrosis type. Areas of slow conduction can be triggers for AF. For the simulated 1 mm electrodes, only patchy fibrosis caused signal fractionation. Bearing the similar conduction behavior in mind, a method to detect diffuse fibrosis would be valuable for AF treatment. Campos et al. [4] have shown, that microelectrodes might be able to detect fractionation from such fine structures. Another outcome is the strongly decreased signal amplitude for a VFr above 40 %, were still conduction was present. This type of 'electrically silent' area of slow conduction if present in vivo could bear a potential as unnoticed AF trigger. Compared to our clinical CFAE signal database our simulations displayed similar characteristics as CFAE classes 1 and 2. The shorter time between zero crossings might be linked to our high initial CV. Smaller simulated signal amplitudes are a result of the chosen method for calculation of extracellular potentials in combination with the chosen conductivity values, which was also seen in [6]. Future work will include further effects linked to CFAE genesis as wavefront collision and uncoupled muscular fibers. Furthermore effects of remodelling have to be taken into account.

Table 2. Characteristic features extracted from simulated signals for different VFr of patchy fibrosis; Values in brackets: electrode distance in mm

	PPA	NM	TM	NZC	TZC
0 (1)	1.07	2.00	7.00	2.00	5.00
0 (3)	1.22	2.00	8.00	2.00	6.00
0 (5)	0.92	2.00	10.00	2.00	8.00
30 (1)	0.12	2.00	9.00	4.00	5.00
30 (3)	0.08	5.00	3.25	4.00	6.67
30 (5)	0.06	4.00	5.67	3.00	8.00
40 (1)	0.02	6.00	5.20	5.00	5.75
40 (3)	0.02	7.00	4.33	7.00	4.33
40 (5)	0.02	5.00	6.50	7.00	4.67
50 (1)	0.01	7.00	7.17	8.00	4.43
50 (3)	0.01	8.00	5.29	8.00	5.86
50 (5)	0.01	8.00	5.86	10.00	4.67

References

[1] Nademanee K, McKenzie J, Kosar E, Schwab M, Sunsaneewitayakul B, Vasavakul T, Khunnawat C, Ngarmukos T. A new approach for catheter ablation of atrial fibrillation: mapping of the electrophysiologic substrate. Journal of the American College of Cardiology 2004;43:2044–2053. ISSN 0735-1097.

[2] Spach MS, Heidlage JF, Dolber PC, Barr RC. Mechanism of origin of conduction disturbances in aging human atrial bundles: experimental and model study. Heart Rhythm Feb 2007;4(2):175–85.

[3] Jacquemet V, Henriquez CS. Genesis of complex fractionated atrial electrograms in zones of slow conduction: a computer model of microfibrosis. Heart Rhythm Jun 2009; 6(6):803–10.

[4] Campos F, Wiener T, Prassl A, Weber Dos Santos R, Sanchez-Quintana D, Ahammer H, Plank G, Hofer E. Electro-anatomical characterization of atrial microfibrosis in a histologically detailed computer model. IEEE Trans Biomed Eng Apr 2013;.

[5] Schilling C. Analysis of Atrial Electrograms (Karlsruhe transactions on biomedical engineering) (Volume 17). KIT Scientific Publishing, 2012. ISBN 978-3-86644-894-0.

[6] Keller MW, Schuler S, Seemann G, Dössel O. Differences in intracardiac signals on a realistic catheter geometry using mono and bidomain models. In Computing in Cardiology, volume 39. Krakow, 2012; 305–308.

[7] Courtemanche M, Ramirez RJ, Nattel S. Ionic mechanisms underlying human atrial action potential properties: Insights from a mathematical model. Am J Physiol 1998;275:H301–H321.

[8] de Jong S, van Veen TA, van Rijen HV, de Bakker JM. Fibrosis and cardiac arrhythmias. Journal of Cardiovascular Pharmacology 2011;57(6):630–638.

[9] Nguyen MP, Schilling C, Dössel O. A new approach for automated location of active segments in intracardiac electrograms. In IFMBE Proceedings World Congress on Medical Physics and Biomedical Engineering, volume 25/4. 2009; 763–766.

Address for correspondence:
KIT- Intstitute of Biomedical Engineering, Matthias Keller
Fritz-Haber-Weg 1, 76131 Karlsruhe, Germany
publications@ibt.kit.edu